Arch. Pharm. Res. (2020) 43:242–256
https://doi.org/10.1007/s12272-020-01221-6

Online ISSN 1976-3786
Print ISSN 0253-6269

Archives of Pharmacal Research
www.springer.com/12272

RESEARCH ARTICLE

Plumbagin engenders apoptosis in lung cancer cells *via* caspase-9 activation and targeting mitochondrial-mediated ROS induction

Surya Kant Tripathi[1] · Kannan R. R. Rengasamy[2] · Bijesh Kumar Biswal[1]

Received: 28 August 2019 / Accepted: 27 January 2020 / Published online: 7 February 2020

Abstract Plumbagin is a naturally-derived phytochemical which exhibits promising medicinal properties, including anticancer activities. In the present study, the anticancer potential of plumbagin has been demonstrated in lung cancer cells by targeting reactive oxygen species (ROS) and the intrinsic mitochondrial apoptotic pathway. Plumbagin showed impressive cytotoxic, anti-proliferative, and anti-migratory activities with IC_{50} 3.10 ± 0.5 µM and 4.10 ± 0.5 µM in A549 and NCI-H522 cells, respectively. Plumbagin treatment significantly reduced the size of A549 tumor spheroids in a concentration-dependent manner. Plumbagin enhanced ROS production and arrested lung cancer cells in S and G2/M phase. Expression of antioxidant genes such as glutathione S-transferase P1 and superoxide dismutase-2 were found to be upregulated with plumbagin treatment in A549 cells. Plumbagin induced dissipation in mitochondrial membrane potential and affected the expression of intrinsic apoptotic pathway proteins. Increased expression of cytochrome c promotes the activation of pro-apoptotic protein Bax with decreased expression of anti-apoptotic protein Bcl-2. Further, plumbagin activated the mitochondrial downstream pathway protein caspase-9 and caspase-3 leading to apoptosis of A549 cells. Collectively, plumbagin could be a promising future phytotherapeutic candidate for lung cancer treatment via targeting intrinsic mitochondrial apoptotic pathway and ROS.

✉ Bijesh Kumar Biswal
biswalb@nitrkl.ac.in

[1] Cancer Drug Resistance Laboratory, Department of Life Science, National Institute of Technology Rourkela, Rourkela, Odisha 769008, India

[2] Department of Bioresource and Food Science, Konkuk University, Seoul 05029, South Korea

Keywords Plumbagin · Lung cancer · Phytotherapeutics · Apoptosis · Mitochondrial membrane potential · Reactive oxygen species

Introduction

Lung cancer is currently the prevailing frightening morbidity and mortality, leading to cancer—related death throughout the world. To date, cases of lung cancer are increasing very frequently worldwide, reckoning 1.38 million deaths annually (Miller et al. 2016). The current treatment choices for lung cancer are chemotherapy, radiotherapy, and sometimes surgery. These treatment options for lung cancer are inadequate because of severe side effects and the development of resistance to therapy (Heavey et al. 2014). Therefore, search for novel therapeutics having lesser side effects and more potent anti-lung carcinogenic effect is highly needed.

Apoptosis is a highly regulated biochemical event in multicellular organisms that lead to the elimination of undesired cells by phagocytosis. It is crucial for development and plays a protective role against tumor cells in human beings (Letai 2017). However, dysregulation of the apoptotic mechanism has a direct link with many diseases of human, including cancer (Letai 2017). Mitochondria have a prominent role in cancer cell death via depolarization in their membrane potential (Kalainayakan et al. 2018). There are differences between mitochondria of normal and cancerous cells, which might be a cause of deregulated reactive oxygen species (ROS) metabolism in cancer cells (Wang et al. 2017).

Phytochemicals have the potential to kill cancer cells selectively because of their deregulated ROS metabolism (Huang et al. 2018; Maheswari et al. 2018). Targeting the effect of potent phytochemicals on the ROS level in cancer cells is one of the most exciting subjects of research in the

anti-cancer world. Caspases and Bcl-2 family proteins are the key regulator of apoptosis through intrinsic mitochondrial apoptotic pathway (Lee et al. 2012). Caspase-9 is one of the key members of the caspase family plays a dominant role in the intrinsic mitochondrial apoptotic pathway mediated cell death (Kim et al. 2015). Cell culture assay has its long history for study in cancer but, most of the time, unable to mimic model organisms, which lack the accurate evaluation of the biological performance of drugs (Edmondson et al. 2014; Katt et al. 2016). Therefore, the generation of tumor spheroid models could be a possible solution to fill the gap between the cell culture assay and model organisms.

Natural products play a very prominent role in the treatment of many human diseases, including cancer. The application of natural products as an anticancer drug is a powerful approach to find a novel biologically active anticancer molecule. Therefore, the present study is focused on a yellow crystalline naphthoquinone-derivative phytochemical named plumbagin (5-hydroxy-2-methyl-1, 4-naphthoquinone), isolated and purified compound of *Plumbago zeylanica* L. plant roots (Jamal et al. 2014). Plumbagin exhibits potent antiproliferative, anti-angiogenic, anti-invasive, and apoptotic property in many human cancers (Cao et al. 2018; Tripathi et al. 2019). It has been documented that plumbagin promotes cytotoxicity in cancer cells by accumulating ROS (Xu and Lu 2010), which influences the depletion of mitochondria membrane potential (MMP) leading to mitochondrial stress. However, plumbagin induced ROS accumulation and its effect on intrinsic mitochondrial-apoptotic pathway proteins in lung cancer cells remains vague. Therefore, this study was designed to elucidate the plumbagin induced cytotoxicity via targeting intrinsic mitochondrial-apoptotic pathway proteins and ROS accumulation in lung cancer cells.

Material and methods

Chemicals and antibodies

Sigma-Aldrich Chemical Co. (St. Louis, MO, USA) provided us phytochemical Plumbagin (5-Hydroxy-2-methyl-1, 4-naphthoquinone), Carbonyl cyanide m-chlorophenylhydrazone (CCCP), Dichloro-dihydro-fluorescein diacetate (DCFH-DA), and Rhodamine-123. Procurement of staining dyes including 4′,6-diamidino-2-phenylindole (DAPI), Ethidium bromide (EtBr), (4,5-dimethylthiazol-2-yl)-2,5-diphenyl tetrazolium bromide (MTT), and Propidium iodide (PI), Acridine orange (AO), and chemicals including Dimethyl sulfoxide (DMSO), N-acetylcysteine (NAC), Ribonuclease-A, and Triton X-100 were done from Hi-Media Laboratories, Mumbai, India. Apoptosis detection kit was brought from ABGENEX Pvt. Ltd., Bhubaneswar, Odisha, India. Antibodies such as Bax, Bcl-2, β-actin, caspase-9/cleaved caspase-9, cleaved caspase-3, and cytochrome c were purchased form ABGENEX Pvt. Ltd., Bhubaneswar, Odisha, India.

Cell culture

We are grateful to the National Center for Cell Science (NCCS, Pune, India) to provide us human lung cancer cells named A549 and NCI-H522. Both the lung cancer cells were grown in Dulbecco's Modified Eagle Medium (DMEM) (Gibco/Invitrogen, Grand Island, New York, USA) supplemented with 10% (v/v) Fetal Bovine Serum (FBS) (Gibco/Invitrogen, Grand Island, New York, USA), 1X antibiotic–antimycotic (Gibco/Invitrogen, Grand Island, New York, USA), and l-Glutamine (Gibco/Invitrogen, Grand Island, New York, USA). The cells were kept in 95% air humidified, 5% CO_2 incubator at 37 °C, and sub-cultured in 70–80% confluent monolayer condition with 0.25% trypsin–EDTA (Gibco/Invitrogen, Grand Island, New York, USA). Plumbagin was disolved in DMSO and freshly diluted in DMEM during experiment performed.

Cell viability assay

Both A549 and NCI-H522 cells (7.5×10^3 cells in each well) were seeded in 96 well plate. After overnight incubation, plumbagin treatment was done in both the cells with concentrations 0, 1, 2, 3, 4, 5, and 6 µM for 24 h. Control cells were treated DMSO with (0.05%) mixed in DMEM. After treatment, 4 h incubation of A549 and NCI-H522 cells were done with MTT in the dark. Then, the solubilizing agent was added and took the absorbance at 570 nm in ELISA plate reader (Synergy-H1microplate reader, Biotek, USA). The cell viability percentage was calculated as follows-

$$\% \text{ cell viability} = \frac{\text{Absorbance of treated cells}}{\text{Absorbance of control cells (0.05\% DMSO)}}$$

Morphological assessment assay

A549 and NCI-H522 (3×10^5 cells) were seeded in 35 mm plate for overnight. After overnight incubation, plumbagin treatment was done in both the lung cancer cells for 24 h. Then, changes in cell morphology were imaged under an inverted phase-contrast microscope (Olympus, Hamburg, Germany).

Tumour spheroid development from cancer cells

Multicellular tumor spheroids show very much similarity with in-vivo tumors, including morphology, growth, proliferation, etc. Therefore, we generated the multicellular tumor spheroids of A549 lung cancer cells in 96 well

plates. 2.5×10^4 cells were seeded in 2% w/v agar pre-coated 96 well plate and incubated at 37 °C in 5% CO_2 incubator with 95% humidity for 48 h. During incubation, cells were aggregated and formed a 3D spheroid structure. Then, spheroids of almost similar and uniform sizes were selected for the further plumbagin treatment. Moreover, spheroids were treated with a desired concentration of plumbagin (0, 3, and 5 µM) for 24 h. Moreover, changes in size (area, μm^2) were observed and imaged at 0 and 24 h of plumbagin treatment under an inverted phase-contrast microscope (Olympus, Hamburg, Germany), whereas a graph was plotted using software (GraphPad Prism 5.0 software, California Corporation, USA).

Clonogenic assay

A549 and NCI-H522 (5×10^2 and 1×10^3 cells, respectively) were seeded in 6 well plate for overnight. Plumbagin treatment was done for 24 h in both the lung cancer cells and then cultured for 21 days with constant media change in every 3 days. On the 21st day, cells were fixed in methanol followed by PBS wash and stained with crystal violet dye for 15 min. Then, each well was gently washed with water and left overnight for air drying. Afterward, colonies having more than 50 cells were reckoned under an inverted phase-contrast microscope (Olympus, Hamburg, Germany), and a graph was plotted using software (GraphPad Prism 5.0 software, California Corporation, USA).

Scratch-invasion assay

A549 (3×10^5 cells) cell suspension were seeded in 6 well plate and kept for overnight incubation, and then cells were kept at serum starvation conditions for 24 h. A linear scratch wound was created by a 1 ml sterile tip followed by washing with PBS to remove the cell debris from the wells. Treatment with plumbagin was done at different concentrations. The scratch healing rate was observed and imaged at 0, 24, and 48 h with the help of an inverted phase-contrast microscope (Olympus, Hamburg, Germany).

Nuclear staining of cells for apoptosis detection

AO/EtBr staining

A549 and NCI-H522 (3×10^5 cells) were treated with the specified concentration of plumbagin for 24 h. Cells were trypsinized, pellet down, and re-suspended in serum-free DMEM. After that, dye mixture AO (100 µg/ml) / EtBr (100 µg/ml) was added in each tube in 1:1 ratio and kept for 5 min in the dark at room temperature. Subsequently, cells were mixed, and 10 µl of the sample from each tube was taken, put on a glass slide and then, examined and imaged under a fluorescence microscope (Olympus, Hamburg, Germany).

DAPI staining

A549 and NCI-H522 (3×10^5 cells) were seeded in 6 well plate and incubated overnight. Plumbagin treatment was done for 24 h, and then cells were fixed in 2% formaldehyde for 15 min. Both the cells were stained with DAPI (1 µg/ml), followed by PBS wash for 30 min in the dark. After that, cells were washed in PBS twice and immediately observed and imaged under a fluorescence microscope (Olympus, Hamburg, Germany).

Annexin V-FITC/PI staining

Plumbagin induced apoptosis in lung cancer cells was detected by an apoptosis detection kit using a flow cytometer. A549 (1×10^5 cells) was seeded in 12 well plate and incubated overnight, afterward treated with plumbagin for 24 h. The control and treated cells were trypsinized, pellet down, and washed in PBS. Then, both control and treated cells were re-suspended in 100 µl of binding buffer containing 5 µl Annexin V-FITC and 5 µl PI. Cells were mixed properly, and incubated for 20 min in the dark at room temperature. After that, 400 µl of additional binding buffer was added in each tube, and plumbagin induced apoptosis was determined in a flow cytometer (BD Accuri™ C6, California, USA).

Intracellular ROS measurement

A fluorescent probe DCFH-DA was used to measure the changes in intracellular ROS level by fluorescence microscopy and flow cytometry. Briefly, A549 and NCI-H522 (1×10^5 cells) were seeded in 12 well plate and kept for overnight incubation. After incubation, plumbagin treatment was done for 24 h. Then, for microscopic fluorescence analysis, cells were stained with 20 µM DCFH-DA followed by PBS wash for 45 min in the dark. Finally, cells were observed and imaged under a fluorescence microscope (Olympus, Hamburg, Germany) for change in the intracellular ROS level. However, for flow cytometric analysis, cells were trypsinized and re-suspended in 20 µM DCFH-DA containing serum-free media and incubated 45 min in the dark. Then, changes in the intracellular ROS level were observed in a flow cytometer (BD Accuri™ C6, California, USA).

Assessment of mitochondrial membrane potential

Variation in mitochondrial membrane potential (MMP) was detected through a fluorescence microscope and flow cytometer using Rhodamine-123 stain. CCCP (a standard MMP

alleviating agent) used as a positive control to confirm the membrane potential reducing property of plumbagin in lung cancer cells. In brief, A549 and NCI-H522 cells were seeded in 12 well plate and kept for overnight incubation. Plumbagin treatment was done at 0, 3, 5 µM concentrations for 24 h. After that, treated cells were fixed in 70% ethanol, followed by PBS wash. For microscopic fluorescence analysis, cells were incubated with fluorescent probe rhodamine-123 (10 µg/ml) and incubated 20 min in the dark at 37 °C. While for flow cytometry analysis, cells were trypsinized and washed with PBS and then re-suspended in fluorescent probe rhodamine-123 (10 µg/ml) and incubated 20 min in the dark at 37 °C. Then fluorescence microscopy (Olympus, Hamburg, Germany) and flow cytometery (BD Accuri™ C6, California, USA) analysis were done.

Quantitative real-time PCR (qPCR)

The effect of plumbagin treatment on the basal mRNA expression of antioxidant genes in the lung cancer cell line (A549) was quantified by real-time PCR analysis. A549 cells were plated in 6 well plate, and treatment of plumbagin was done at 0, 3, 5 µM concentrations for 24 h. Then, total cell RNA was isolated using TRI reagent (Molecular Research Center Inc. USA). 2 µg of total RNA was converted into cDNA using High Capacity cDNA Reverse Transcription Kit (Applied Biosystems, Thermo Fisher Scientific, Baltics UAB, Vilnius). The synthesized cDNA product was used for expression analysis of antioxidant genes such as glutathione S-transferase P1 (GSTP1) and superoxide dismutase-2 (SOD-2) with reference to housekeeping gene GAPDH using GoTaq qPCR Master Mix (Promega, San Luis Obispo, CA, USA) in Real-Time PCR System (Eppendorf, New York, USA). Sequence details of primers used in the study are given in Table 1.

Western blotting

A549 and NCI-H522 cells were treated with the desired concentrations (0, 3, and 5 µM) of plumbagin for 24 h. Then, cells were washed with pre-cooled PBS, and total cell protein lysates were homogenized using RIPA lysis buffer having 1X proteinase K inhibitor (Promega, San Luis Obispo, CA, USA). After that, protein lysates were harvested and quantified using the BCA protein estimation kit. Then equal amount of control and treated protein lysates (40 µg/ml) were separated on polyacrylamide gel electrophoresis. After separation the proteins were transferred to nitrocellulose membrane (Hi-Media Laboratories, Mumbai, India) and then membrane blocking was done in 5% non-fat milk powder for 1 h. Nitrocellulose membrane was exposed to primary antibodies for overnight at 4 °C. Then, washing of the membrane was done in TBST thrice for 10 min each, after that exposed to secondary antibody conjugated with HRP for 2 h at room temperature. In all the experiments, β-actin was used as an endogenous control. Finally, bands were developed on X-ray film with the help of a chemiluminescence solution (Amersham™ ECL™ Western Blotting Analysis System, GE Healthcare, UK).

Statistical analysis

All the experimental data and statistical differences were analyzed by GraphPad Prism 5.0 software, California Corporation, USA. The data with probability (p) value < 0.05 were considered as statistically significant. The standard deviation (SD) was represented in the form of error bars, as mean $\pm$ SD of three independent experiments.

Results

Plumbagin induces cytotoxicity in lung cancer

To find cytotoxic potential of plumbagin in lung cancer cells (A549 and NCI-H522), plumbagin treatment was done at various concentrations (0, 1, 2, 3, 4, 5, and 6 µM) for 24 h (Fig. 1a). Our finding revealed that plumbagin treatment in both A549 and NCI-H522 cells inhibited the growth of cells at IC_{50} values less than 5 µM. The half-maximal cytotoxic concentrations (IC_{50}) of plumbagin for A549 and NCI-H522 cells are given in Fig. 1b and c. However, A549 cells showed more sensitivity towards plumbagin as compared to NCI-H522 cells. Subsequently, plumbagin induced morphological changes were revealed that both lung cancer cells exhibiting nuclear condensation at 3 µM of treatment for 24 h. At 5 µM concentration of plumbagin, cells appeared like membrane blebbing, detached from the plate, and floating in the media (Fig. 1d). Treatment of plumbagin in multicellular tumor spheroid of A549 cells significantly reduced the spheroid size (area; μm^2) in a concentration-dependent manner

Table 1 Sequences of primers used in the study

Gene	Forward primer	Reverse primer
GAPDH	5′-GCAAGGGTGCGTCCTATG-3′	5′-AGAGTGTGGGTGGGTAGTGT-3′
GSTP1	5′-TACACCAACTATGAGGCGGG-3′	5′-AGCGAAGGAGATCTGGTCTC-3′
SOD2	5′-GTTGGCCAAGGGAGATGTTAC-3′	5′-AGCAACTCCCCTTTGGGT TC-3′

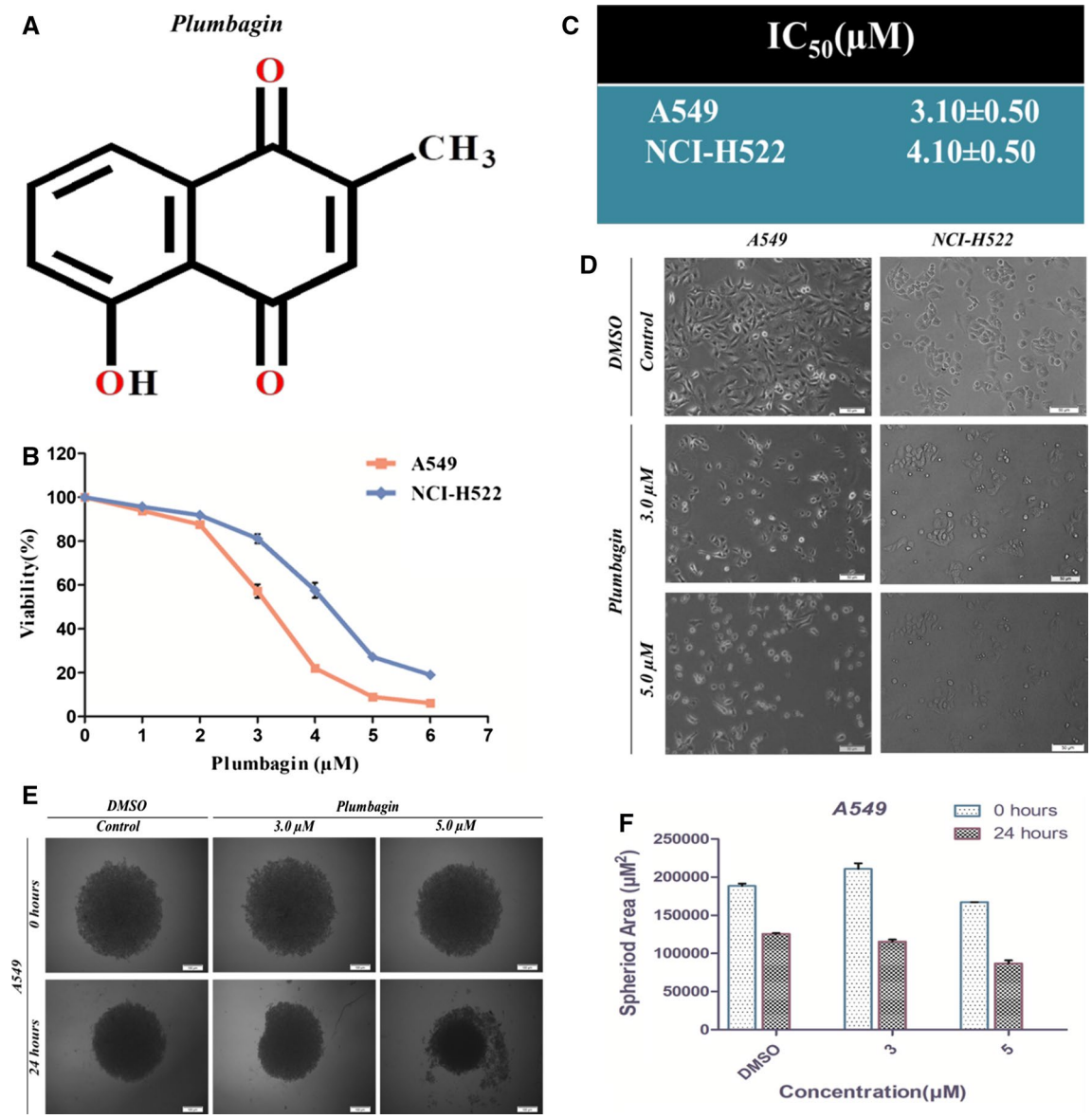

Fig. 1 Effect of plumbagin on the viability of lung cancer cells (A549 and NCI-H522). **a** Structure of phytochemical plumbagin. **b** Histogram showing cell viability of A549 and NCI-H522 cells treated with plumbagin 0, 1, 2, 3, 4, 5, and 6 μM concentrations for 24 h through MTT assay. **c** Plumbagin's IC_{50} values for A549 and NCI-H522 cells were calculated using GraphPad Prism 5.0 software, California Corporation, USA. **d** Observed the change in the morphology of A549 and NCI-H522 cells treated with plumbagin (0, 3, 5 μM) for 24 h compared to control through an inverted microscope (Olympus, Hamburg, Germany). **e**, **f** Size (area) reducing property of plumbagin in A549 cells tumor spheroid at 24 h in a concentration-dependent manner. DMSO (0.05%) in DMEM media was used as a control for treated cells. Error bars based on mean ± SD of three independent experiments

(Fig. 1e, f). The tumor spheroids size was found to be less than half as compared to untreated spheroids at 5 μM of plumbagin treatment. This finding indicates that plumbagin may have tumor size reducing property in lung cancer. DMSO (0.05%) was used as a control for treatment. Overall, we can conclude that plumbagin has promising cytotoxic and anti-tumorigenic nature in lung cancer cells.

Plumbagin inhibits proliferation and migration of lung cancer cells

Proliferation and migration inhibitory properties of plumbagin in lung cancer cells (A549 and NCI-H522) were assessed through single-cell colony-forming and in-vitro scratch motility assays, respectively. As shown in Fig. 2a and b, plumbagin inhibited the single-cell colony-forming

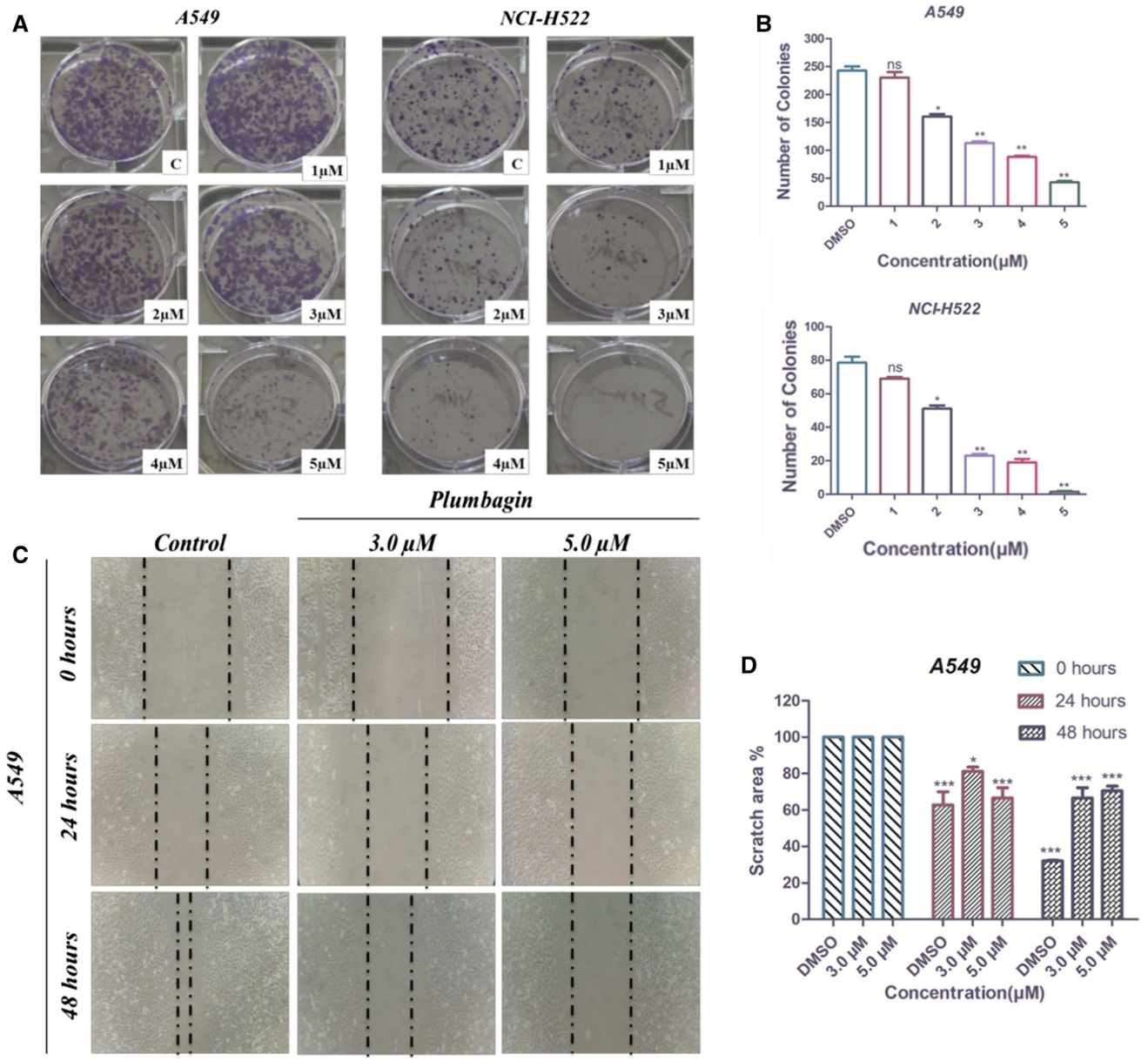

Fig. 2 Plumbagin suppressed the proliferation and metastasis of lung cancer cells. **a**, **b** The single-cell colony-forming ability of A549 and NCI-H522 cells were decreased in contrast to increasing treated concentration (1, 2, 3, 4, and 5 μM) of plumbagin for 24 h. **c**, **d** The migration rate of the A549 cell line was inhibited from the edge of the wound towards the center of the wound by plumbagin treatment (0, 3, and 5 μM) for 24 h compared to control. DMSO (0.05%) in DMEM media was used as a control for treated cells. Images were photographed, and data were analyzed with an inverted microscope (Olympus, Hamburg, Germany) and GraphPad Prism 5.0 software, California Corporation, USA, respectively. Error bars based on mean ± SD of three independent experiments. ***P < 0.001; **P < 0.01; *P < 0.05; and *ns* non-significant, compared to control

ability of lung cancer cells with increasing concentrations of plumbagin treatment. At 5 μM concentration of plumbagin treatment, very few colonies were observed in both A549 and NCI-H522 cells. Further, in-vitro scratch motility assay revealed that plumbagin treatment inhibited the mobility and migration in both A549 and NCI-H522 cells with increasing concentrations of plumbagin treatment (Fig. 2c, d) as compared to control. Overall, these findings highly supported the anti-proliferative and anti-migratory potential of plumbagin in lung cancer.

Plumbagin induces apoptosis in lung cancer

To demonstrate the involvement of plumbagin in inducing apoptosis in A549 and NCI-H522 cells, we performed AO/EtBr, DAPI, and Annexin V-FITC/PI staining. Figure 3a

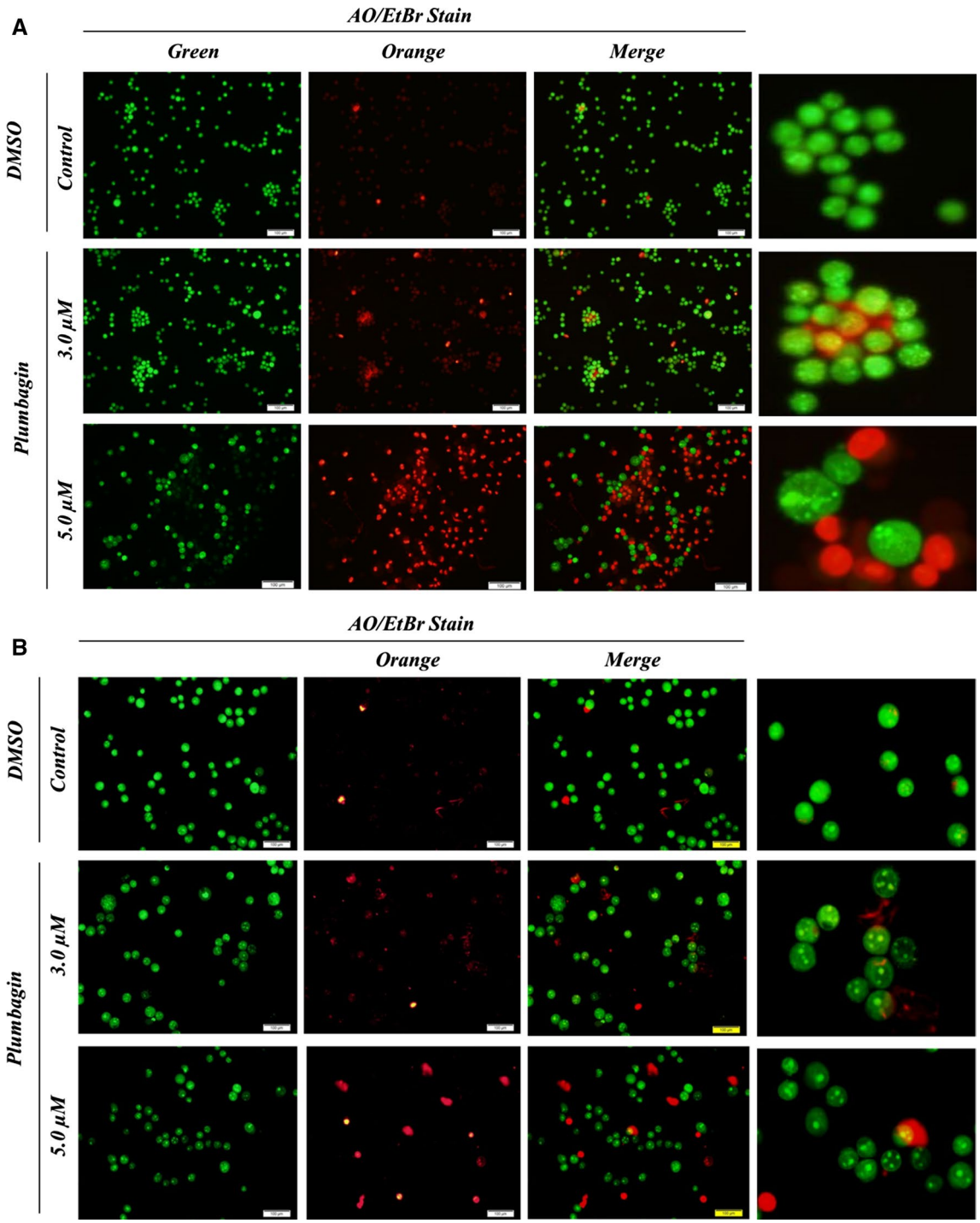

Fig. 3 Plumbagin induces apoptosis in A549 and NCI-H522 lung cancer cells. Both the lung cancer cells A549 and NCI-H522 were treated with plumbagin at concentrations 0, 3, and 5 µM for 24 h. **a, b** AO/EtBr staining showed the cellular morphology of **a** A549, and **b** NCI-H522 cells in viable, early apoptotic, late apoptotic, and necrotic conditions. **c** The nuclear morphology changes were observed by DAPI staining in A549 and NCI-H522 cells. **d** Plumbagin induced apoptotic cells percentage and impact of ROS scavenger (NAC; 10 mM) on plumbagin induced apoptosis in A549 and NCI-H522 cells by Annexin V-FITC/PI staining. All the results were analyzed and captured under a fluorescence microscope (Olympus, Hamburg, Germany)

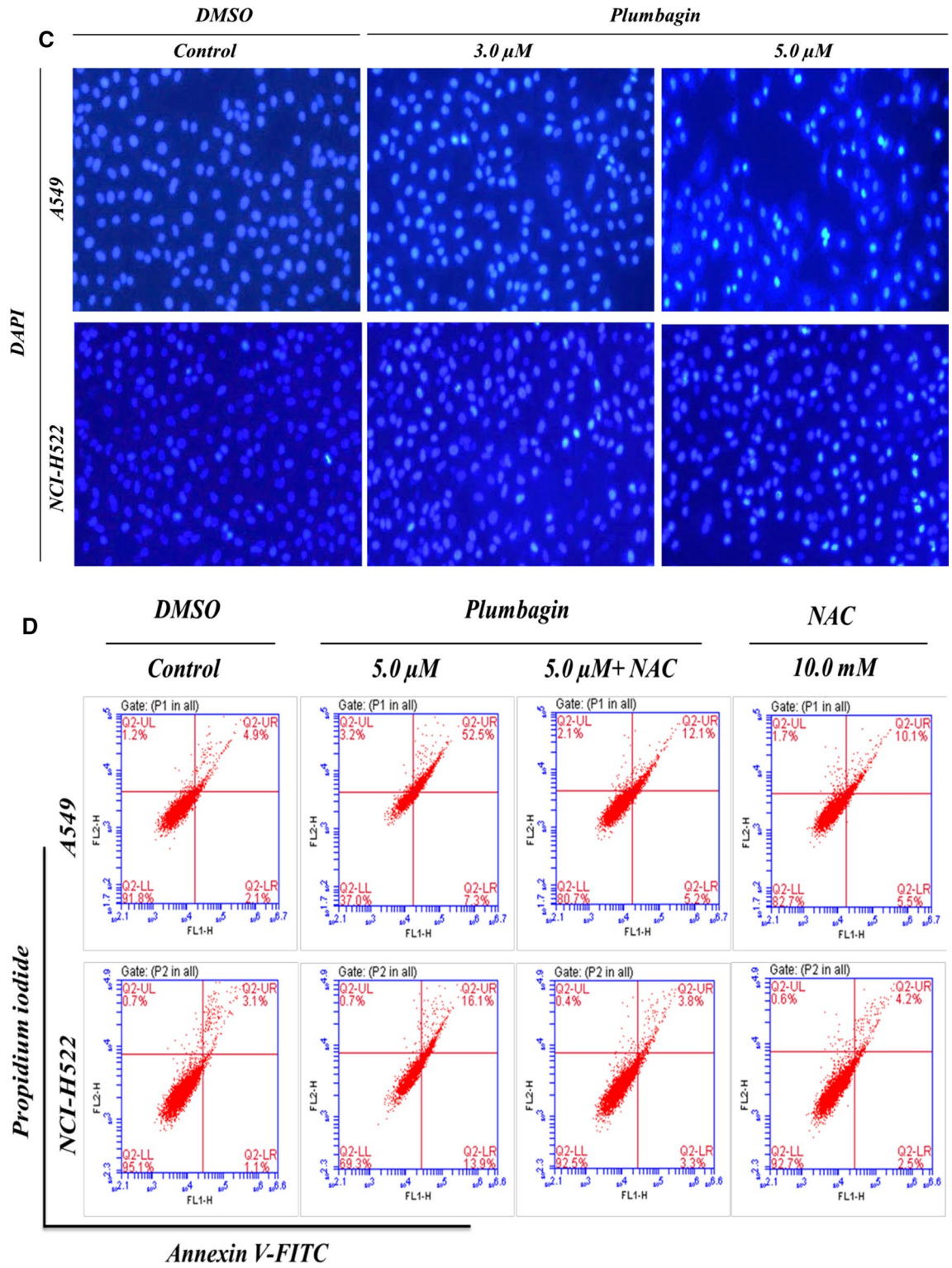

Fig. 3 (continued)

and b have shown normal and plumbagin treated lung cancer cells stained with AO/EtBr stain. Plumbagin treatment (0, 3, and 5 μM) followed by AO/EtBr staining showed increased number of bright green dots, orange-nuclear dots, and red-stained cells with increasing concentration of plumbagin treatment in both A549 and NCI-H522 cells. While

control cells were stained uniformly green in color. Plumbagin treated A549, and NCI-H522 cells showed bright blue fluorescent dots in the center, which indicated the distorted and damaged nuclear morphology of the cells (Fig. 3c). The number of these bright blue fluorescent dots were increased with increasing concentration of plumbagin.

To verified the apoptotic rate of plumbagin in lung cancer cells, Annexin V-FITC/PI staining was done, followed by flow cytometry (Fig. 3d). As compared to control, the apoptotic rate was significantly higher in plumbagin treated A549 and NCI-H522 cells. The apoptotic rates in A549 and NCI-H522 cells treated with the higher dose of plumbagin were observed 59.8% and 30.0%, respectively, which was significantly higher as compared to control (A549 and NCI-H522 cells showing apoptotic rate 7.0% and 4.2%, respectively). To further check the ROS mediated apoptotic property of plumbagin, a ROS scavenger named N-acetyl cysteine (NAC; 10 mM) was used alone and in combination with plumbagin. Interestingly, the use of NAC in combination with plumbagin significantly inhibited the plumbagin cytotoxicity in A549 and NCI-H5499 cells. The apoptotic rates in A549 cells after alone NAC and plumbagin with NAC combination treatment were 15.6% and 17.3%, respectively. Similarly, apoptotic rates in NCI-H522 cells after alone NAC and plumbagin with NAC combination treatment were 3.8% and 7.1%, respectively. Overall, these findings strongly supported the anti-proliferative, anti-migratory, and apoptotic nature of plumbagin via ROS generation in lung cancer cells.

Plumbagin arrests lung cancer cells cell cycle progress

Next, we explored the effect of plumbagin on cell cycle distribution in lung cancer cells using PI stain followed by flow cytometry. According to Fig. 4a–d, 24 h treatment of plumbagin induced S to G2/M and S phase accumulation of A549 and NCI-H522 cells, respectively. Moreover, the combined treatment of NAC with plumbagin reversed the plumbagin mediated cell cycle phase arrest of A549 and NCI-H522 cells (Fig. 4a–d). The overall finding concluded that plumbagin induced cell cycle arrest of lung cancer cells was ROS mediated, which modulated the cell cycle distribution.

Plumbagin induces cell death via ROS in lung cancer cells

To further explore and establish a direct relationship between plumbagin and ROS, DCFH-DA staining was demonstrated in A549 and NCI-H522 cells. NAC (10 mM) was used as a negative control in all the experiments. As shown in Fig. 5a and c, the intensity of green fluorescence were significantly increased with increasing concentration of plumbagin in plumbagin treated A549 and NCI-H522 cells as compared to control cells. While NAC (10 mM) alone or combination of plumbagin and NAC treatment significantly suppressed the green fluorescent intensity in A549 and NCI-H522 cells. Moreover, flow cytometry analysis also demonstrated almost similar results as fluorescence microscopy. Figure 5b and d have shown that peaks of plumbagin treated A549 and NCI-H522 cells are shifted towards the right as compared to control. Further, cell viability assay confirmed that use of NAC (10 mM) and plumbagin combination did not show any cytotoxicity in both A549 and NCI-H522 cells (Fig. 5e, f). These findings concluded that plumbagin induced excess ROS production in lung cancer cells, thereby cell death of lung cancer cells.

Plumbagin induces intrinsic mitochondrial apoptotic pathway and activates caspase-9/3

Additionally, we demonstrated the effect of plumbagin on mitochondrial membrane potential using Rhodamine-123 dye. CCCP (100 μM) was used as a positive control in all the experiments given in Fig. 6. The microscopic fluorescence analyses (Fig. 6a) have shown that the green fluorescent intensity was significantly suppressed by plumbagin treatment (0, 3, and 5 μM) in A549 and NCI-H522 cells with increasing concentrations. In CCCP (100 μM) treated A549 and NCI-H522 cells, green fluorescent intensity was also reduced as compared to untreated cells. Further, we confirmed the fluorescence microscopy results of plumbagin induced mitochondrial-mediated apoptotic effect via flow cytometry in both A549 and NCI-H522 cells (Fig. 6b, c). It has been clearly shown that MMP peaks of plumbagin and CCCP treated cells were shifted towards left of the control cells with increasing concentrations. Shifting of peaks of plumbagin and CCCP treated A549 and NCI-H522 cells compared to control cells, highly supported the depletion in MMP of lung cancer cells. Further, we demonstrated the effect of plumbagin on the expression of antioxidant genes (GSTP1 and SOD2) in A549 cells using qRT-PCR analysis. The experimental findings suggested that plumbagin treatment for 24 h at desired concentrations enhanced the expression of antioxidant genes such as GSTP1 and SOD2 in A549 cells with increasing concentrations (Fig. 6d, e). Due to the induction of ROS in these cells, they upregulated the antioxidant enzymes; which might play a role in resistance to plumbagin in A549 cells. Subsequently, we examined the expression of Bcl-2 family proteins in A549 cells involved in intrinsic mitochondrial-mediated apoptosis by western blot analysis (Fig. 6f, g). Our findings suggested that plumbagin treatment enhanced the pro-apoptotic protein Bax expression and suppressed the expression of anti-apoptotic protein Bcl-2 in A549 cells. Also, plumbagin increased the expression level of cytochrome c as per concentration-dependent manner.

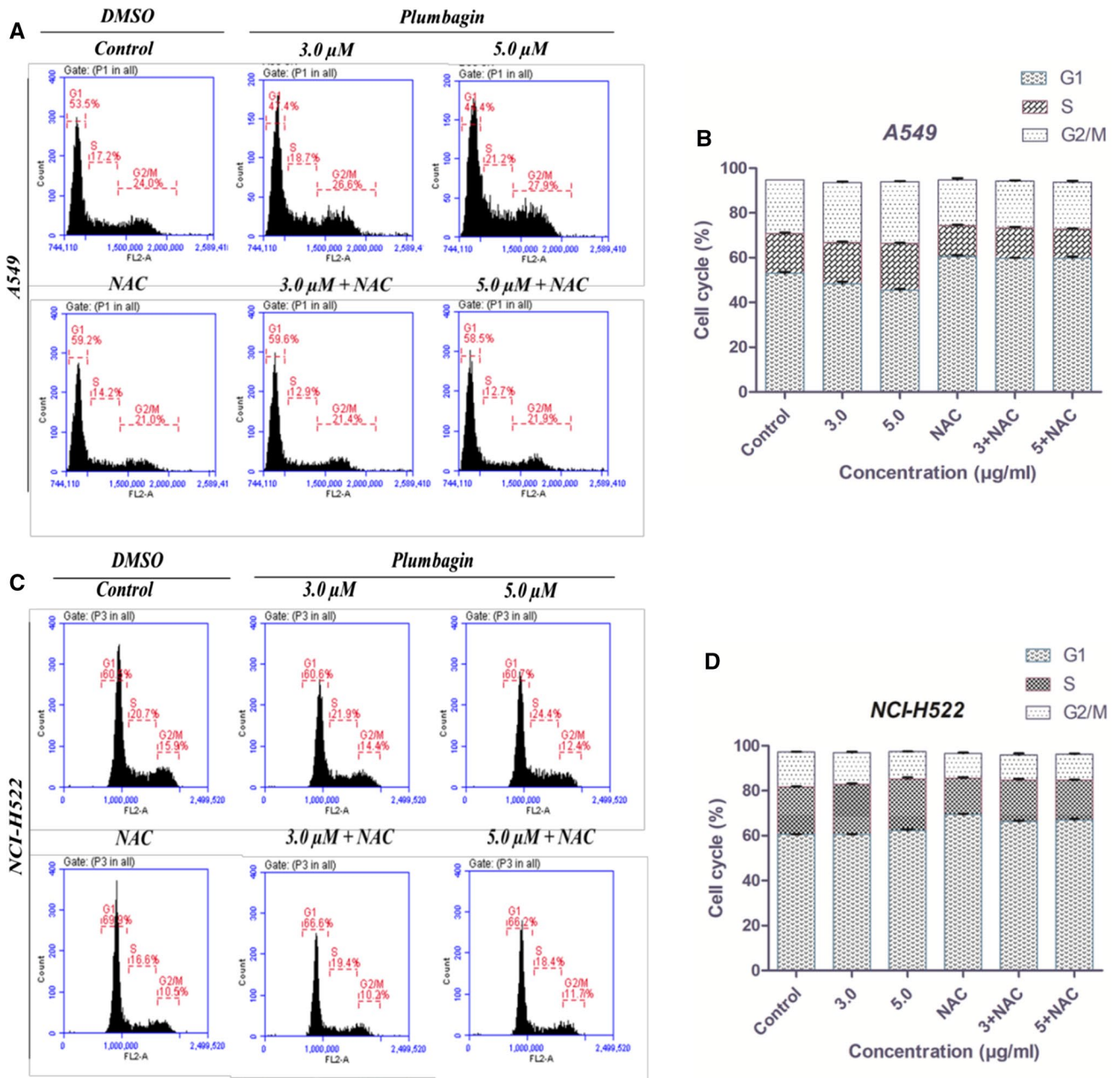

Fig. 4 Plumbagin arrests the A549 and NCI-H522 lung cancer cells in the G2/M phase. Both the lung cancer cells A549 and NCI-H522 were treated with plumbagin concentrations 0, 3, and 5 μM; NAC (10 mM); and plumbagin + NAC for 24 h. **a**, **c** Representative data showed cell cycle distribution with PI staining followed by flow cytometry analysis of A549 and NCI-H522 cells. **b**, **d** The histograms are showing G1, S, and G2/M phase distribution of A549 and NCI-H522 cells from three separate experimental analyses. Error bars based on mean ± SD of three independent experiments

Further, plumbagin treatment in A549 cells activated the caspase-9 with further activation of downstream intrinsic apoptotic protein caspase-3 as per increasing concentrations (Fig. 6f, g). In conclusion, plumbagin induced cell death in lung cancer cells through excess ROS production, depletion in MMP, and activation of intrinsic mitochondrial apoptotic pathway protein caspase-9/3.

Discussion

To date, phytochemicals have an enormous research interest in the treatment of many diseases, including cancer (Tripathi and Biswal 2018). Plumbagin is a naphthoquinone analog which shows cytotoxicity against many cancer cells. Therefore, our present study has believed that plumbagin possesses promising anticancer properties in lung cancer

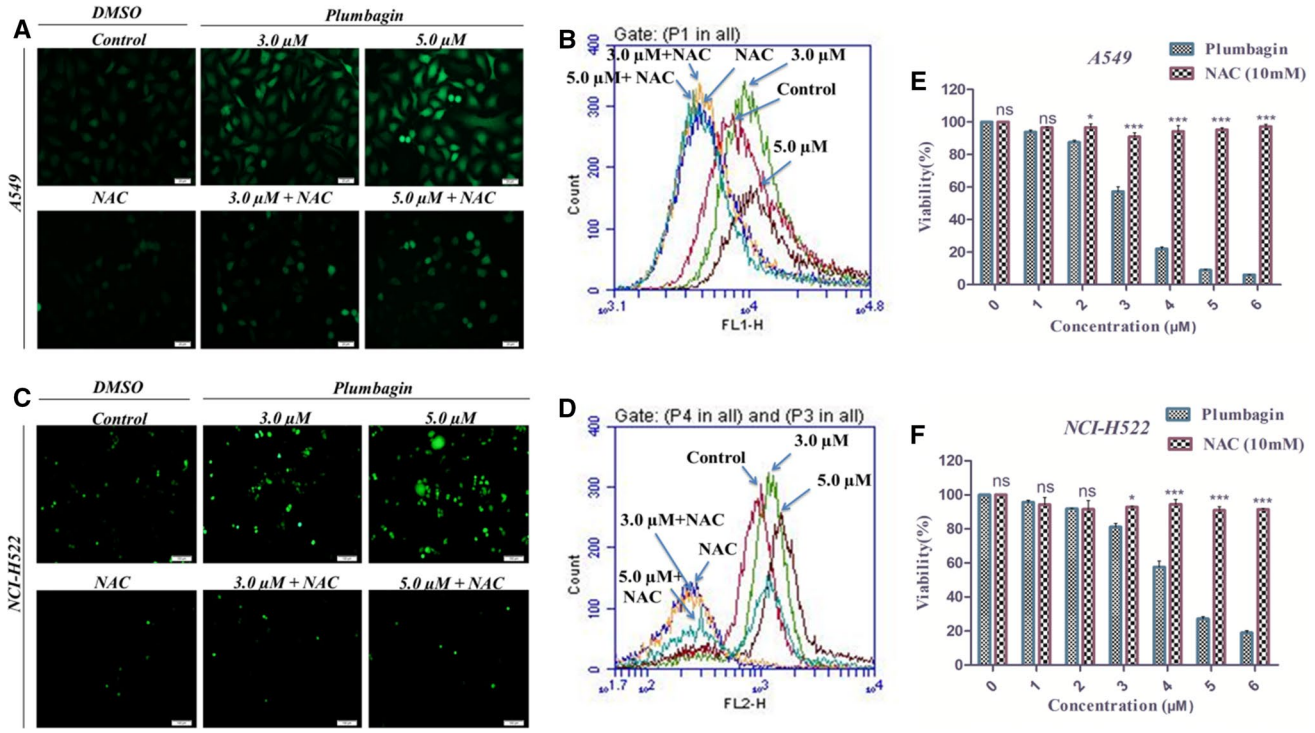

Fig. 5 ROS accumulation after plumbagin treatment in lung cancer cells A549 and NCI-H522, thereby induction of apoptosis. Both the lung cancer cells A549 and NCI-H522 were treated with plumbagin concentrations 0, 3, and 5 μM; NAC (10 mM); and plumbagin + NAC for 24 h. **a**, **c** Representative data show ROS accumulation with DCFH-DA staining followed by microscopic fluorescence analysis, **b**, **d** by flow cytometry analysis in A549 and NCI-H522 cells. **e**, **f** Histograms of cell viability assay to prove plumbagin induced cytotoxicity mediated by excess ROS production in A549 and NCI-H522 cells. Treatment of plumbagin + ROS scavenger (NAC) did not show cytotoxicity in A549, and NCI-H522 cells confirmed ROS mediated cytotoxicity by plumbagin. Error bars based on mean ± SD of three independent experiments. ***$P < 0.001$

cells (A549 and NCI-H522). Plumbagin has been known to induce apoptosis in many cancers through ROS production (Xu et al. 2013; Cao et al. 2018). Here, we demonstrated the experimental evidence to confirm the ROS mediated anticancer potential of plumbagin in lung cancer cells. Our present study revealed that plumbagin has strong cytotoxic potential and apoptosis induction property in lung cancer cells (A549 and NCI-H522) at a very low concentration from 0 to 6 μM. Also, plumbagin inhibited the growth of both A549 and NCI-H522 cells at IC_{50} value less than 5 μM at 24 h of treatment. However, A549 cells showed more sensitivity towards plumbagin compared to NCI-H522. Previously, Inbaraj et al. study documented that plumbagin IC_{50} dose for human normal Keratinocytes cells HaCaT was 18 μM. Interestinglty, the cytotoxic IC_{50} dose of plumbagin for human normal Keratinocytes cells was much higher than the observed cytotoxic IC_{50} dose against lung cancer cells used in our study (Inbaraj and Chignell 2004). Therefore, we can conclude that plumbagin may use as a therapeutic against lung cancer cells in clinical studies. Morphological changes itself, provide a clear indication of apoptosis (Maheswari et al. 2018). Observation of plumbagin treated lung cancer cells changed its morphologies including cell shrinkage, initiate detaching from the plate, cytoplasmic condensation, and floated in the media compared to control. It has been observed that tumor spheroids show similarity with tumor microenvironment conditions in solid cancer, which work as an excellent ex vivo model for anti-cancer drug screening (Benien and Swami 2014). We also found that treatment of plumbagin significantly reduced the size and area of lung tumor spheroids. These findings conclude that plumbagin has promising cytotoxic and therapeutic potential against lung cancer.

Reports have been suggested that apoptosis is a well-regulated biological process that maintains a balance between cell survival and death (Huang et al. 2018). Deregulation of the apoptotic pathway favors cancer initiation, progression, and metastasis. We observed that plumbagin effectively inhibited single-cell colony-forming ability and migration rate of lung cancer cells (A549 and NCI-H522). Staining of plumbagin treated lung cancer cells with AO/EtBr showed bright green, orange-nuclear, and red color dots, which indicated the early apoptotic, late apoptotic, and necrotic phase, respectively (Pajaniradje et al. 2014; Afsar et al. 2016). Furthermore, plumbagin promoted the distortion and damage

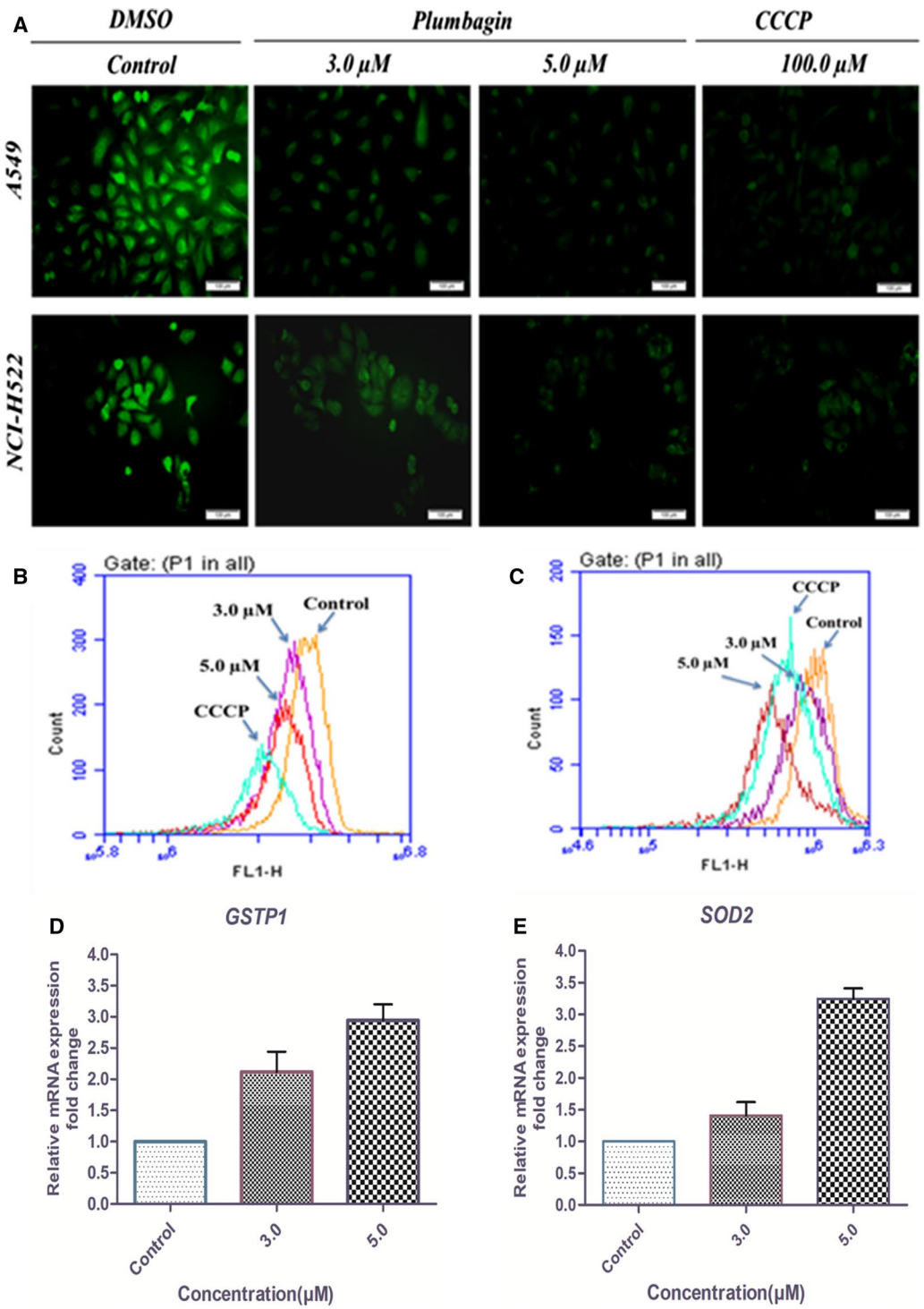

Fig. 6 Plumbagin treatments cause oxidative stress and activate the intrinsic mitochondrial apoptotic pathway in lung cancer. Both the lung cancer cells A549 and NCI-H522 were treated with plumbagin concentrations (0, 3, and 5 μM) and CCCP concentration (100 μM) for 24 h, followed by Rhodamine-123 staining. Representative data showed reduced green fluorescence with increased concentration of plumbagin treatment with Rhodamine-123 staining; **a** followed by microscopic fluorescence analysis, and **b**, **c** followed by flow cytometry of A549 and NCI-H522 cells compared to control. **d**, **e** The fold change in mRNA expression of antioxidant genes (GSTP1 and SOD2) in plumbagin treated A549 cell line after 24 h were determined by qRT-PCR. **f**, **g** Western blotting to analyzed plumbagin exposure effect on the expression of intrinsic mitochondrial apoptotic proteins (Bax, Bcl-2, Caspase-9, and caspase-3) after 24 h of treatment. β-actin was used as a loading control for all the proteins. Error bars based on mean ± SD of three independent experiments

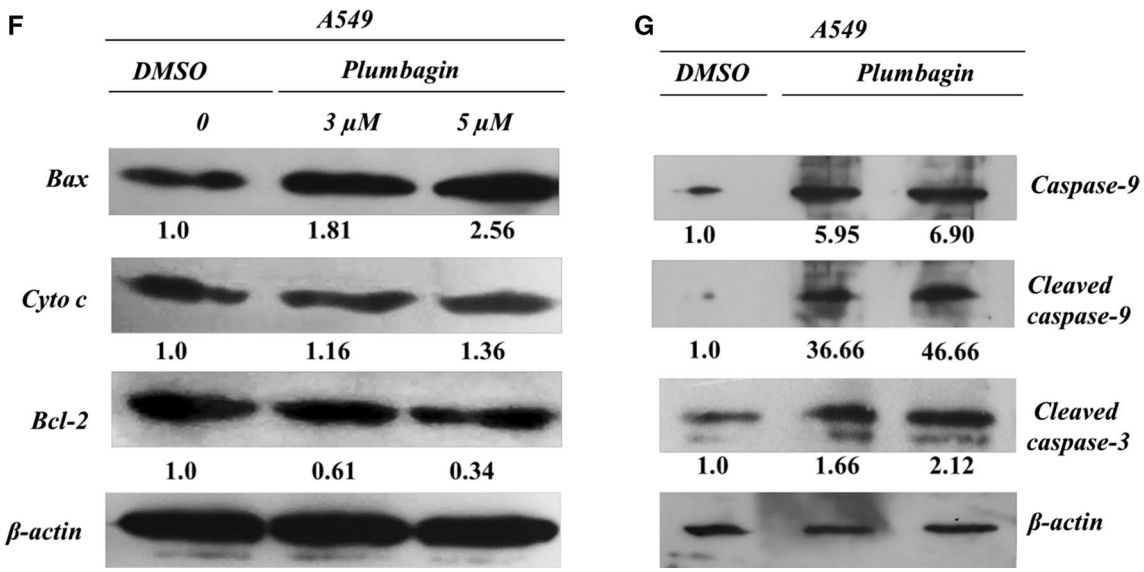

Fig. 6 (continued)

of nuclear morphology with increasing concentration in A549 and NCI-H522 cells. Therefore, we could conclude that increased concentration of plumbagin induced pre-apoptosis, late apoptosis, and necrosis in A549 and NCI-H522 cells.

Indeed, ROS is a double-edged sword because high ROS may cause severe oxidative damage, thereby cell death, while it may also induce carcinogenesis by activating oncogenes and DNA mutations (Asadi-Samani et al. 2019). Studies suggested that cancer cells produce ROS more abundantly than normal cells, which helps them to flourish more as compared to normal cells (Asadi-Samani et al. 2019). In our study, Annexin-V FITC/PI staining of control and plumbagin treated A549, and NCI-H522 cells showed the cytotoxic nature of plumbagin with concentration-dependent manner. Simultaneously, the use of a well-known ROS scavenger (NAC) in combination with plumbagin significantly reversed the apoptotic effect of plumbagin in both A549 and NCI-H522 cells. These findings strongly recommended the anti-proliferative, anti-migratory, and apoptotic nature of plumbagin via enhanced ROS production.

Our and many other previous studies showed that phytochemicals restrict the growth of cancer cells by cell cycle arrest (Maheswari et al. 2018; Tripathi and Biswal 2018). Similarly, plumbagin has also been documented to arrest the cancer cells in particular cell cycle phase in many cancer types, including esophageal cancer (Cao et al. 2018), pancreatic cancer (Wang et al. 2015), prostate cancer (Qiu et al. 2015), colon cancer (Eldhose et al. 2014), etc. Our findings demonstrated that plumbagin arrested the A549 in G2/M and S phase and NCI-H522 cells in only the G2/M phase. Combined treatment of NAC and plumbagin showed reversion of plumbagin induced cell cycle arrest of lung cancer cells. Therefore, we could conclude that plumbagin induced cell cycle arrest is ROS mediated.

Intrinsic mitochondrial-dependent apoptotic pathway is one of the significant deregulated pathways in many cancers (Czabotar et al. 2014; Huang et al. 2018). Moreover, the intrinsic mitochondrial apoptotic pathway has been regulated by many factors, and change in the expression of cytoplasmic Bcl-2 family proteins is one of them (Czabotar et al. 2014). Oxidative stress such as excess ROS production and mitochondrial stress are inducing factors for the activation of the intrinsic mitochondrial-dependent apoptotic pathway. One of the previous studies indicated the antioxidant activity of plumbagin, but this study was only based on biochemical estimation (Tilak et al. 2004). Through our experimental results, we found that plumbagin enhanced the expression of antioxidant genes such as GSTP1 and SOD2 with concentration-dependent manner. These findings conclude the oxidative stress-inducing property of plumbagin in lung cancer cells. Previous reports suggested that severe ROS production promotes mitochondrial stress resulting in loss of MMP (Hua et al. 2015). Our results strongly recommended that plumbagin enhanced the ROS production in lung cancer cells, which resulted in depletion in MMP. High expression of pro-apoptotic protein Bax helps in the downregulation of anti-apoptotic protein Bcl-2 expression, which may enhance the permeability of the mitochondrial membrane, thereby activation of caspase-9/3 (Lee et al. 2012). We found that plumbagin treatment upregulated the expression of Bax protein and suppressed the expression of Bcl-2 protein, thus activation of caspase-9. Indeed, activation of caspase-9 further activated caspase-3 protein, thereby

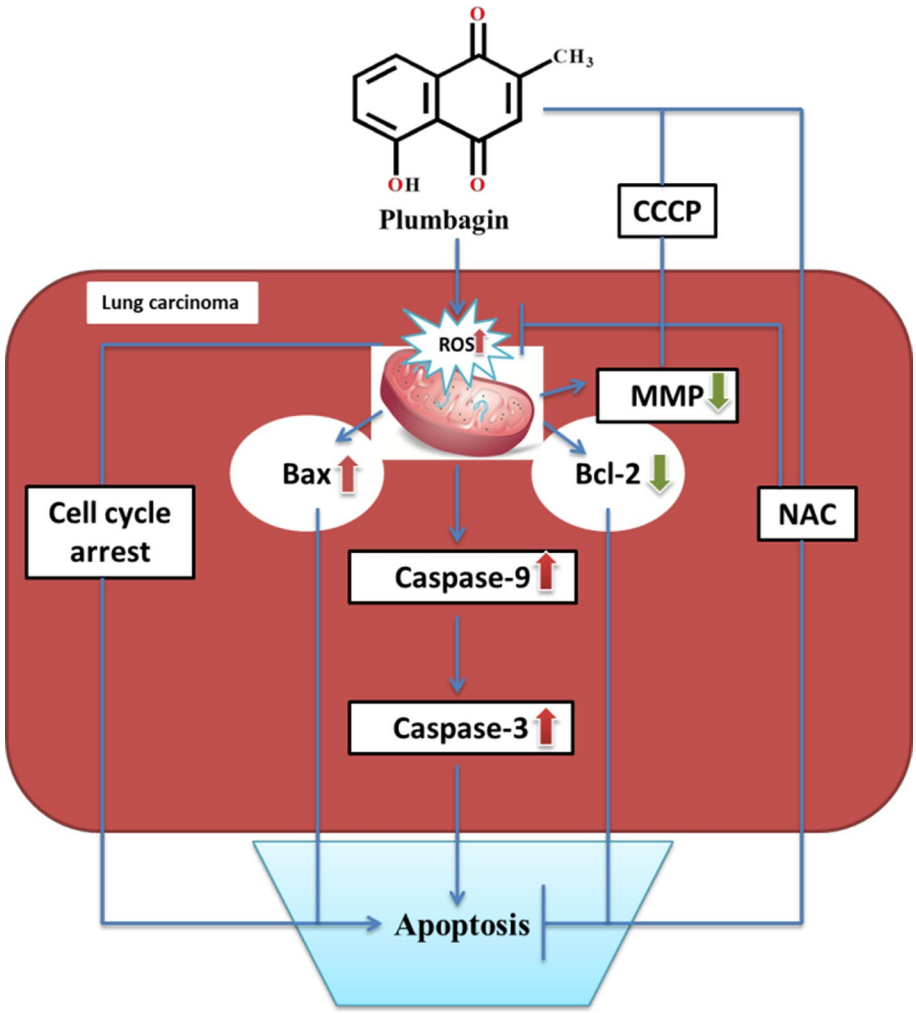

Fig. 7 Schematic summary of plumbagin induced cytotoxicity and involved mechanisms to induced apoptosis in lung cancer cells

mitochondrial mediated apoptosis of cancer cells (Jin et al. 2017). Figure 7 summarized plumbagin induced cytotoxicity and involved mechanisms in apoptosis of lung cancer cells. In conclusion, plumbagin induces cell death of lung cancer cells through intrinsic mitochondrial-dependent apoptotic pathway, depletion in mitochondrial membrane potential, and promoted excess ROS production. Overall, we conclude that plumbagin may be used as an future anti-lung cancer agent after rigorous clinical and pre-clinical studies.

References

Afsar T, Trembley JH, Salomon CE, Razak S, Khan MR, Ahmed K (2016) Growth inhibition and apoptosis in cancer cells induced by polyphenolic compounds of *Acacia hydaspica*: involvement of multiple signal transduction pathways. Sci Rep 6(1):23077. https://doi.org/10.1038/srep23077

Asadi-Samani M, Farkhad NK, Mahmoudian-Sani MR, Shirzad H (2019) Antioxidants as a double-edged sword in the treatment of cancer antioxidants. IntechOpen. https://doi.org/10.5772/intechopen.85468

Benien P, Swami A (2014) 3D tumor models: history, advances and future perspectives. Future Oncol 10(7):1311–1327. https://doi.org/10.2217/fon.13.274

Cao YY, Yu J, Liu TT, Yang KX, Yang LY, Chen Q, Shi F, Hao JJ, Cai Y, Wang MR (2018) Plumbagin inhibits the proliferation and survival of esophageal cancer cells by blocking STAT3-PLK1-AKT signaling. Cell Death Dis 9(2):17. https://doi.org/10.1038/s41419-017-0068-6

Czabotar PE, Lessene G, Strasser A, Adams JM (2014) Control of apoptosis by the BCL-2 protein family: implications for physiology and therapy. Nat Rev Mol Cell Biol 15(1):49. https://doi.org/10.1038/nrm3722

Edmondson R, Broglie JJ, Adcock AF, Yang L (2014) Three-dimensional cell culture systems and their applications in drug discovery and cell-based biosensors. Assay Drug Dev Technol 12(4):207–218. https://doi.org/10.1089/adt.2014.573

Eldhose B, Gunawan M, Rahman M, Latha MS, Notario V (2014) Plumbagin reduces human colon cancer cell survival by inducing cell cycle arrest and mitochondria-mediated apoptosis. Int J Oncol 45(5):1913–1920. https://doi.org/10.3892/ijo.2014.2592

Heavey S, Godwin P, Baird AM, Barr MP, Umezawa K, Cuffe S, Finn SP, O'Byrne KJ, Gately K (2014) Strategic targeting of the PI3K–NFκB axis in cisplatin-resistant NSCLC. Cancer Biol Ther 15(10):1367–1377. https://doi.org/10.4161/cbt.29841

Hua P, Sun M, Zhang G, Zhang Y, Tian X, Li X, Cui R, Zhang X (2015) Cepharanthine induces apoptosis through reactive oxygen

species and mitochondrial dysfunction in human non-small-cell lung cancer cells. Biochem Biophys Res Commun 460(2):136–142. https://doi.org/10.1016/j.bbrc.2015.02.131

Huang TC, Chiu PR, Chang WT, Hsieh BS, Huang YC, Cheng HL, Huang LW, Hu YC, Chang KL (2018) Epirubicin induces apoptosis in osteoblasts through death-receptor and mitochondrial pathways. Apoptosis 23(3–4):226–236. https://doi.org/10.1007/s1049

Inbaraj JJ, Chignell CF (2004) Cytotoxic action of juglone and plumbagin: a mechanistic study using HaCaT keratinocytes. Chem Res Toxicol 17(1):55–62. https://doi.org/10.1021/tx034132s

Jamal MS, Parveen S, Beg MA, Suhail M, Chaudhary AG, Damanhouri GA, Abuzenadah AM, Rehan M (2014) Anticancer compound plumbagin and its molecular targets: a structural insight into the inhibitory mechanisms using computational approaches. PLoS ONE 9(2):e87309. https://doi.org/10.1371/journal.pone.0087309

Jin Y, Fan JT, Gu XL, Zhang LY, Han J, Du SH, Zhang AX (2017) Neuroprotective activity of cerebrosides from *Typhonium giganteum* by regulating caspase-3 and Bax/Bcl-2 signaling pathways in PC12 cells. J Nat Prod 80(6):1734–1741. https://doi.org/10.1021/acs.jnatprod.6b00954

Kalainayakan SP, FitzGerald KE, Konduri PC, Vidal C, Zhang L (2018) Essential roles of mitochondrial and heme function in lung cancer bioenergetics and tumorigenesis. Cell Biosci 8(1):56. https://doi.org/10.1186/s13578-018-0257-8

Katt ME, Placone AL, Wong AD, Xu ZS, Searson PC (2016) In vitro tumor models: advantages, disadvantages, variables, and selecting the right platform. Front Bioeng Biotechnol 4:12. https://doi.org/10.3389/fbioe.2016.00012

Kim B, Srivastava SK, Kim SH (2015) Caspase-9 as a therapeutic target for treating cancer. Expert Opin Ther Targets 19(1):113–127. https://doi.org/10.1517/14728222.2014.961425

Lee JH, Won YS, Park KH, Lee MK, Tachibana H, Yamada K, Seo KI (2012) Celastrol inhibits growth and induces apoptotic cell death in melanoma cells via the activation ROS-dependent mitochondrial pathway and the suppression of PI3K/AKT signaling. Apoptosis 17(12):1275–1286. https://doi.org/10.1007/s10495-012-0767-5

Letai A (2017) Apoptosis and cancer. Annu Rev Cancer Biol 1:275–294. https://doi.org/10.1146/annurev-cancerbio-050216-121933

Maheswari U, Ghosh K, Sadras SR (2018) Licarin A induces cell death by activation of autophagy and apoptosis in non-small cell lung cancer cells. Apoptosis 23(3–4):210–225. https://doi.org/10.1007/s10495-018-1449-8

Miller KD, Siegel RL, Lin CC, Mariotto AB, Kramer JL, Rowland JH, Stein KD, Alteri R, Jemal A (2016) Cancer treatment and survivorship statistics, 2016. CA A Cancer J Clini 66(4):271–289. https://doi.org/10.3322/caac.21349

Pajaniradje S, Mohankumar K, Pamidimukkala R, Subramanian S, Rajagopalan R (2014) Antiproliferative and apoptotic effects of *Sesbania grandiflora* leaves in human cancer cells. BioMed Res Int 2014:474953. https://doi.org/10.1155/2014/474953

Qiu JX, Zhou ZW, He ZX, Zhao RJ, Zhang X, Yang L, Zhou SF, Mao ZF (2015) Plumbagin elicits differential proteomic responses mainly involving cell cycle, apoptosis, autophagy, and epithelial-to-mesenchymal transition pathways in human prostate cancer PC-3 and DU145 cells. Drug Des Dev Ther 2015(9):349–417. https://doi.org/10.2147/DDDT.S71677

Tilak JC, Adhikari S, Devasagayam TP (2004) Antioxidant properties of *Plumbago zeylanica*, an Indian medicinal plant and its active ingredient, plumbagin. Redox Rep 9(4):219–227. https://doi.org/10.1179/135100004225005976

Tripathi SK, Biswal BK (2018) *Pterospermum acerifolium* (L.) wild bark extract induces anticarcinogenic effect in human cancer cells through mitochondrial-mediated ROS generation. Mol Biol Rep 45(6):2283–2294. https://doi.org/10.1007/s11033-018-4390-6

Tripathi SK, Panda M, Biswal BK (2019) Emerging role of plumbagin: cytotoxic potential and pharmaceutical relevance towards cancer therapy. Food Chem Toxicol 125:566–582. https://doi.org/10.1016/j.fct.2019.01.018

Wang F, Wang Q, Zhou ZW, Yu SN, Pan ST, He ZX, Zhang X, Wang D, Yang YX, Yang T (2015) Plumbagin induces cell cycle arrest and autophagy and suppresses epithelial to mesenchymal transition involving PI3K/Akt/mTOR-mediated pathway in human pancreatic cancer cells. Drug Des Dev Ther 2015(9):537–560. https://doi.org/10.2147/DDDT.S73689

Wang JP, Hsieh CH, Liu CY, Lin KH, Wu PT, Chen KM, Fang K (2017) Reactive oxygen species-driven mitochondrial injury induces apoptosis by teroxirone in human non-small cell lung cancer cells. Oncol Lett 14(3):3503–3509. https://doi.org/10.3892/ol.2017.6586

Xu KH, Lu DP (2010) Plumbagin induces ROS-mediated apoptosis in human promyelocytic leukemia cells in vivo. Leukemia Res 34(5):658–665. https://doi.org/10.1016/j.leukres.2009.08.017

Xu TP, Shen H, Liu LX, Shu YQ (2013) Plumbagin from *Plumbago Zeylanica* L induces apoptosis in human non-small cell lung cancer cell lines through NF-κB inactivation. Asian Pac J Cancer Prev 14(4):2325–2331. https://doi.org/10.7314/APJCP.2013.14.4.2325